Research Article | Vol. 28, No. 10 / 11 May 2020 / Optics Express 14922

Optics EXPRESS

Triggering of different pulsed regimes in fiber cavity laser by a waveguide electro-optic switch

BORIS NYUSHKOV,[1,2] ALEKSEY IVANENKO,[1,*] SERGEY SMIRNOV,[1] OLGA SHTYRINA,[1] AND SERGEY KOBTSEV[1]

[1] Novosibirsk State University, 1 Pirogova Str., Novosibirsk 630090, Russia
[2] Novosibirsk State Technical University, 20 Prospekt K. Marksa, Novosibirsk 630073, Russia
[*] ivanenko.aleksey@gmail.com

Abstract: A novel practical method for electronic triggering of essentially different pulsed regimes in fiber cavity lasers is introduced. The method relies on electronic control of complementary transmission characteristics of a fiber-coupled $LiNbO_3$ waveguide electro-optic switch (WEOS) which plays the role of the variable output coupler in a fiber cavity. The method was studied using a testbed laser configuration comprised of a semiconductor optical amplifier (SOA) and an all-fiber cavity. Modulation of the WEOS-based output coupling in the fast gain recovery configuration allowed not only high-quality mode locking and harmonic mode-locking at certain pulse repetition rates determined by the cavity round trip time, but it also allowed nanosecond pulsed output of the same quality to be yielded by cavity dumping at widely and continuously tunable repetition rate (ranging from kHz to MHz). Thus, WEOS-based electronically variable output coupling allows uniquely high flexibility for lasing regimes and characteristics within a single all-fiber cavity configuration.

1. Introduction

Application of electronically controllable fiber components in all-fiber lasers significantly strengthens the advantages of this laser type. To the desirable features of the all-fiber design, which does not require alignment and servicing, are added other benefits: possibility of the electronic management and tuning of different generation regimes. Continued development of photonic technologies leads to establishment of qualitatively new methods of electronic control over laser parameters in all-fiber configurations. For example, among such methods is electrochemical tuning of modulation characteristics in graphene- or carbon-nanotube-based all-fiber saturable absorbers [1,2] used for passive mode locking. Also, of great practical interest are new active methods for electronic triggering of desirable pulsed regimes. These methods were typically advanced by employing original electronically controllable fiber (or fiber-coupled) components, such as for instance all-fiber acousto-optic modulators [3,4], semiconductor amplifier/electro-absorption modulator [5], or microstructured fiber with variable birefringence [6]. We believe, however, that more advanced solutions for active electronic control of pulsed regimes in fiber cavity lasers should rely on usage of fast electro-optic waveguide devices [7,8] which can ensure high modulation capability with low driving voltage as well as commercial availability. Among those devices are waveguide electro-optic switches (WEOS) [9] which can afford more extended control capabilities for the lasers.

The present work stems from the idea of using a fast fiber-coupled WEOS as the laser's output coupler uniquely combining two intracavity elements in one: a variable output coupler and an intensity modulator. WEOS-based all-electronic control of essentially different pulsed lasing regimes (*i.e.* mode locking and cavity dumping) within a single all-fiber cavity configuration is studied here for the first time. To the best of our knowledge, no earlier demonstration of such control implementation and no study of different lasing regimes driven by it were reported so far. The all-fiber cavity dumping demonstrated in [6] was established by using a

#391972 https://doi.org/10.1364/OE.391972
Journal © 2020 Received 16 Mar 2020; revised 26 Apr 2020; accepted 27 Apr 2020; published 1 May 2020

Optics EXPRESS

relatively slow polarizing pulse picker switched by current-induced heating. It produced pulses as long as hundreds of nanoseconds at repetition rates below 1.5 kHz, which were affected by polarization instability. In contrast, a fiber-coupled $LiNbO_3$ WEOS can be nearly as fast as congener waveguide electro-optic intensity modulators [8,10], which are known to be capable of sub-nanosecond laser pulse shaping [11]. This WEOS property along with its polarization insensitive complementary transmission characteristics ushers in new prospects of dynamic electronic control over lasing regimes. The present study explores such control in a fiber cavity laser with the semiconductor active medium which features fast (sub-nanosecond) recovery time as compared to rare-earth-doped fibers. It causes useful lasing features which are discussed along with the potential of the method for other active media.

2. Experimental setup

The experimental laser with an electro-optic coupler is schematically shown in Fig. 1. The laser has a ring-linear fiber cavity configuration similar to our earlier fiber-semiconductor lasers [12]. The new, principal feature is a WEOS-based variable output coupler incorporated into the ring part of the cavity. This part also comprises a fiber-coupled semiconductor optical amplifier (SOA), a reference 1:99 fused fiber coupler, and a fiber circulator (CIR). The latter ensures unidirectional lasing in the cavity ring, and connects it with a fiber Bragg grating (FBG) which prevents broadband multi-wavelength lasing [13]. The FBG has a nearly-1-nm wide reflection spectrum centered at ~1540 nm. Its maximal reflection coefficient is about 0.95. The cavity ring is extended with an optional ~200-m long single-mode fiber (SMF). It reduces the fundamental pulse repetition rate in mode-locked operation to 959 kHz, thereby allowing high-order harmonic mode locking with moderate speed requirements to the control electronics. Thus, mode locking can be sustained both in kHz and MHz domains. The SOA (Thorlabs SOA 1013S) was pumped electrically in the constant current mode (at an operating current of 500 mA). The management of lasing regimes was performed solely by means of the WEOS-based coupler, which was actually a commercial four-port polarization-independent $LiNbO_3$ switch (EOSpace SW-2×2-PI-SFU-SFU-UL). It allows gradual alteration of cross-coupling between the input and output fiber ports by applying control voltage as illustrated in Fig. 2(a). It was controlled by electrical signals from a radiofrequency arbitrary waveform generator (RF AWG, Rigol DG4162) with an effective bandwidth of 40 MHz. Also, there was a facility for adding bias voltage from a direct current (DC) source.

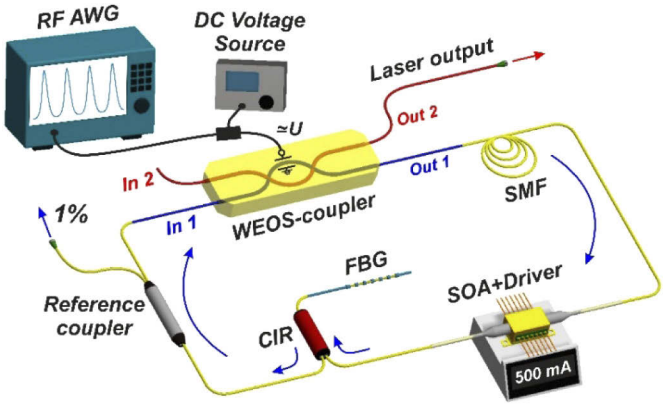

Fig. 1. Schematic diagram of the laser with WEOS-based variable output coupling.

Optics EXPRESS

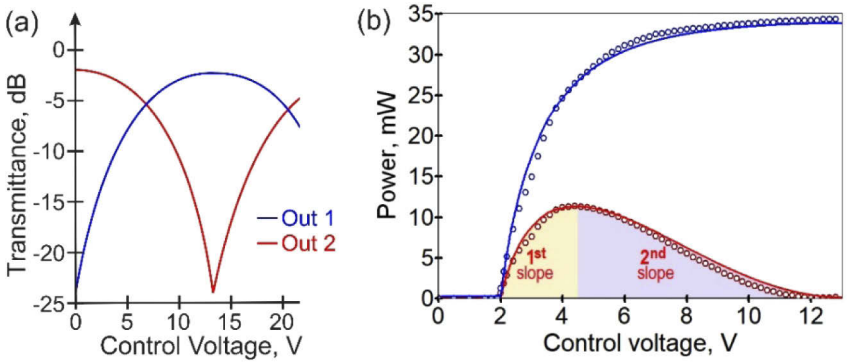

Fig. 2. (a) Voltage dependence of the WEOS complementary optical transmission to the intracavity output port 1 (blue curve) and to the extracavity output port 2 (red curve); (b) Electronically-managed CW power characteristics of the laser: the intracavity laser power sustained at the WEOS input port 1 (blue curve) and the output laser power extracted from the WEOS output port 2 (red curve) versus the control voltage (circles denote experimental data, and solid curves - theoretical data).

3. Electronic control of laser regimes and parameters

3.1. Continuous-wave operation

First, we studied the dependence of continuous-wave (CW) laser performance on varied cross-coupling between the ports of the incorporated WEOS. To this effect, we varied the DC voltage applied to the WEOS, and measured the resulting laser radiation power independently at the WEOS extracavity output port 2 and at the reference coupler's 1% output port. The latter allowed deriving of the intracavity laser power sustained at the WEOS intracavity input port 1. Voltage dependence of the WEOS optical transmission and the resulting laser power characteristics are presented in Fig. 2. The laser performance was scanned within the range of univocal response of the WEOS (0 to 13 V), taking advantage of the full dynamic range of the cross-coupling variation (~22 dB). The zero-voltage state of the WEOS corresponds to the highest optical transmission between its intracavity input port 1 and its extracavity output port 2, thereby introducing the largest intracavity loss. Rising the voltage up to 13 V results in gradual switching of the WEOS optical transmission to the intracavity output port 1, and simultaneous suppression of laser output coupling. The constant (unaffected by the voltage) insertion loss of the WEOS amounts to ~2.4 dB. Taking these characteristics together with the intracavity parasitic losses (totally 3.9 dB) introduced by the other fiber-optic elements, as well as applying the SOA's saturable gain (with the gain coefficient ranging from 18.7 to 6.3 dB), we solved the equation for the gain and loss balance in a stationary lasing regime:

$$\alpha \cdot T_1(U) \cdot g(P) = 1, \tag{1}$$

where $\alpha = 10^{-0.1\times3.9\ \mathrm{dB}} = 0.407$ is the intracavity loss coefficient, $g(P)$ stands for the SOA saturable gain as a function of the SOA exit power P, and $T_1(U)$ is the WEOS intracavity transmittance. The latter was modeled as $T_1(U) = a_0 \cdot \left(\sin^2\left(\frac{\pi}{2}U/\Delta V\right) + \delta\right)$, where U is the control voltage, $\Delta V = 13.0$ V, $a_0 = 10^{-0.1\times2.4\ \mathrm{dB}} = 0.575$ is the WEOS insertion loss, and $\delta = 0.0063$ is a small correction term describing the minimal non-zero coefficient of the WEOS ports coupling. Equation (1) was solved numerically using the bisection method [14], and dependence of the SOA exit power P on the control voltage U was found. To obtain the intracavity laser power entering into the reference 1:99 coupler, we multiplied $P(U)$ by the loss coefficient $\alpha_1 = 10^{-0.1\times1.37\ \mathrm{dB}} = 0.73$ of the cavity segment between the SOA and the

Optics EXPRESS

reference coupler, the result is shown in Fig. 2(b) as a blue solid curve. Then, to obtain laser power at the WEOS output port 2, we multiplied the above calculated intracavity laser power by the reference coupler coefficient, and by the complementary WEOS output transmittance $T_2(U) = a_0 \cdot \left(\cos^2\left(\frac{\pi}{2}U/\Delta V\right) + \delta\right)$, the result is shown in Fig. 2(b) as a red solid curve.

As seen from the above power dependencies, the voltage-induced sweep of the WEOS optical transmission results in a non-monotonic variation of the laser power emitted through the WEOS output port 2. Such variation differs significantly from the behavior of the intracavity laser power as derived from the power measurements at the reference coupler's 1% output port. The lasing threshold is achieved at ~2 V. At voltages in excess of ~5 V, the intracavity power behavior features an evident tendency to saturation. At the same time, the laser power extracted from the WEOS output port 2 reaches the maximum at ~ 4.5 V and then gradually goes down almost to zero as the drive voltage gets increased to ~13 V. This power decay is due to the WEOS switching to the fully intracavity optical transmission. Such laser behavior is qualitatively reproduced even with modified loss and gain parameters.

The discovered feature of partial correlation between the intracavity and output laser powers led us to expect the possibility of triggering essentially different pulsed lasing regimes electronically via the WEOS-based coupler. To generate pulsed output from the WEOS, the control voltage has to be swung within the range of monotonic response (*i.e.* either along the 1st or the 2nd slope of the corresponding power-voltage curve shown in Fig. 2(b)). On this basis we explored two different modes of pulsed operation, as described below.

3.2. Mode-locked pulsed operation

In our experiments, the pulsed operation exploiting the 1st slope of the output power characteristic was driven by a periodic pulsed electrical control signal in the form of 30-ns Gaussian pulses. These electrical pulses were synthesized by means of the RF AWG. They had a positive amplitude of 4.5 V and no bias. Thus, their peak amplitude corresponded to the maximum of the output power characteristic shown in Fig. 2(b). Pulsed lasing emerged when the control pulse repetition rate was adjusted to match the reciprocal of the cavity round trip time (*i.e.* 959.03 kHz) or to its multiple. Detuning from such repetition rate resulted in drastic decrease of the pulsed lasing power to almost zero. Thus, the attainable pulse repetition rate was determined by the cavity round trip time, as is typical of mode-locked lasing.

Figure 3 illustrates the measured basic characteristics of the mode-locked pulse trains alternatively generated at the fundamental repetition rate, and at its 10th harmonics (harmonic mode locking). Time traces (oscillograms) of these pulse trains testify to their good contrast and amplitude stability (root-mean-square (RMS) noise is less than 1%). Their radiofrequency (RF) spectra feature comparatively high signal-to-noise ratios (> 50 dB) at the actual pulse repetition frequencies in the mode-locked and harmonically mode-locked regimes, thereby indicating proper quality of mode locking. It is important to note that the obtained harmonic mode locking features relatively strong suppression of supermode noise (*i.e.* parasitic beats of supermodes appearing at all integer multiples of the fundamental frequency) as seen from the RF spectrum in Fig. 3. The supermode beats are very few dB above the noise floor. Such good suppression of supermode noise is sustained without applying complicated composite cavity configurations [15], solely due to specific features of the SOA saturable gain (especially fast recovery time as compared with Er-fiber gain) [16,17]. This also indicates high stability of modulation parameters, which ensures low timing jitter and amplitude fluctuations of pulses distributed within the cavity period. The laser pulse duration obtained in the mode-locked lasing regime was about 15 ns (at half maximum). Shortening of laser pulses as compared with the control pulse duration mainly occurred due to cutting off the pulse tails that were below the lasing threshold (below the 2 V level). By applying a proper bias voltage one can make laser pulses to approach the duration of control pulses but the biased operation impairs laser noise properties because of weaker

Optics EXPRESS

suppression of parasitic intracavity radiation during the interpulse period. We discovered that the very strong intracavity loss introduced by the unbiased WEOS (in excess of 22 dB) repeatably during each idle (interpulse) period does not even allow sustaining so-called rational harmonic mode locking [18] with the available gain in our laser. On the other hand, the demonstrated mode-locked operation provides very clean pulsed output with remarkably low supermode noise in the harmonic case.

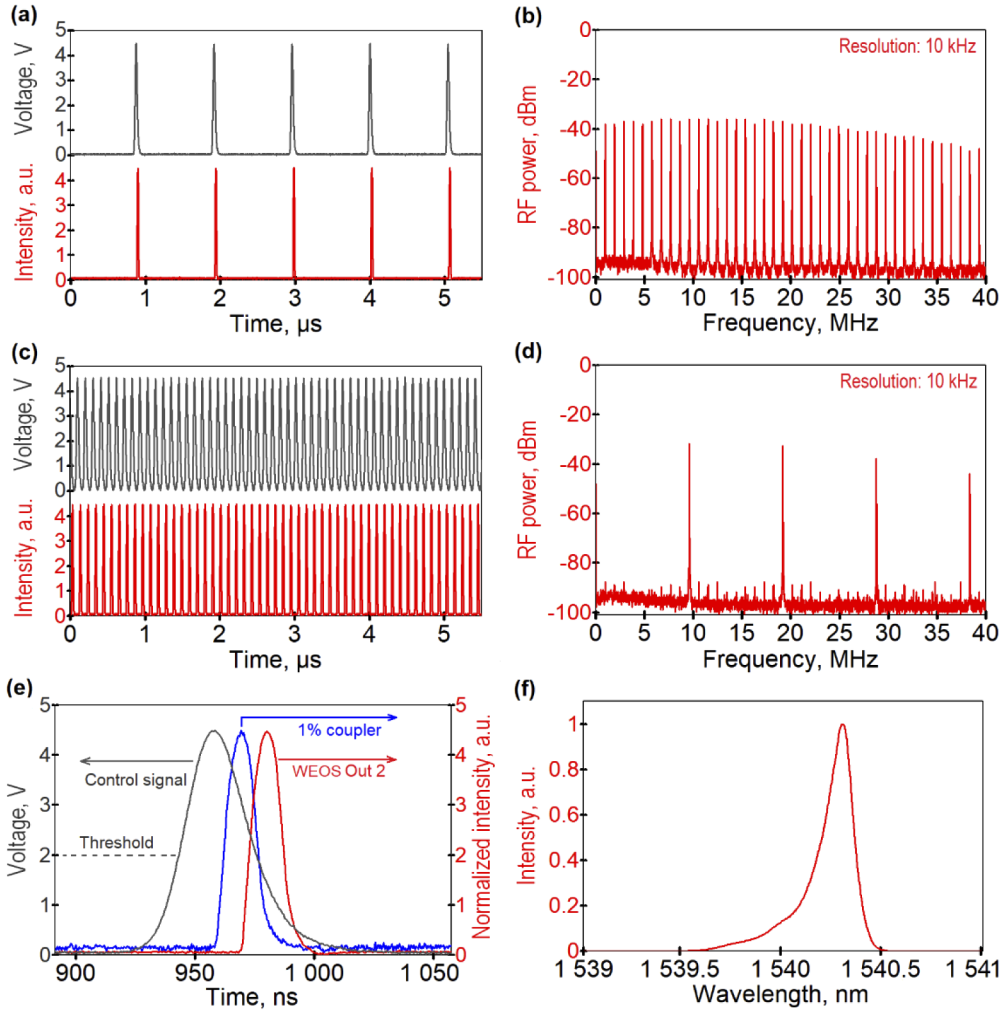

Fig. 3. Measured characteristics of mode-locked and harmonically mode-locked pulsed operations: (a) Oscillogram of electrical control signal (gray trace) and resulting laser pulse train (red trace) driven at the fundamental repetition rate of 959.03 kHz (as imposed by the cavity round trip time); (b) Corresponding RF spectrum of the laser pulse train with the fundamental repetition rate; (c) Oscillogram of electrical control signal (gray trace) and resulting laser pulse train (red trace) driven at the 10^{th} harmonic of the fundamental repetition rate; (d) RF spectrum of the laser pulse train with the 10^{th}-harmonic repetition rate; (e) Typical high-resolution time traces of electrical control pulse (grey trace), laser pulse from the WEOS output port 2 (red trace), and intensity variation at the 1% port of the reference coupler (blue trace); (f) Optical spectrum of laser radiation (resolution 0.02 nm) in mode-locked operation (operations at the fundamental and harmonic repetition rates feature similar spectral profiles).

Optics EXPRESS

The main constraining factor of pulsed operation within the 1st slope is the discrete set of allowed pulse repetition frequencies which is determined by the cavity round trip time. Modulation of the WEOS transmission in this case has to be synchronized with the intracavity circulation of generated laser pulses. Figure 4 illustrates how the mode-locked lasing gets affected by detuning from the proper repetition rate determined by the cavity round trip time. However, pulsed operation within the 2nd slope of the output power characteristic shown in Fig. 2(b) has to be different from the above case, because the output laser power extracted from the WEOS output port 2 turns to be uncorrelated with the nearly-saturated intracavity laser power fed to the WEOS input port 1 when the control voltage exceeds 5 V.

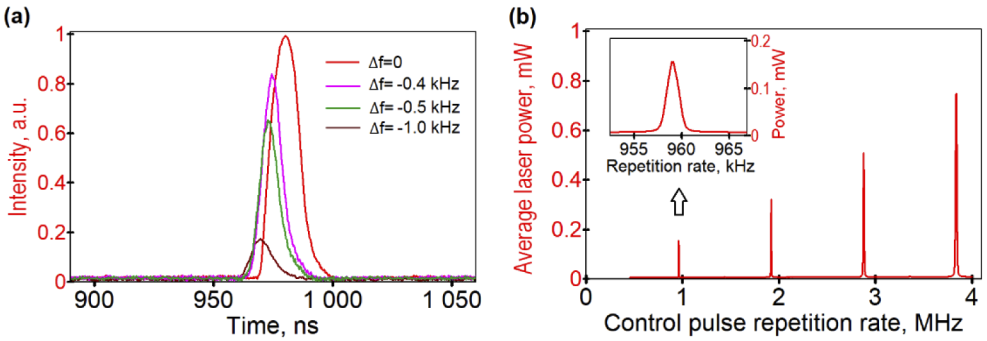

Fig. 4. Impact of the pulse repetition rate detuning on the mode-locked operation: (a) Time traces of laser pulses generated with different extents of mismatch **Δf** between the control signal repetition frequency and the fundamental pulse repetition rate determined by the cavity round trip time; (b) Dependence of the average laser power outputted by the WEOS on the repetition rate of the electrical control pulses (scanned stepwise in increments of 0.5 kHz over the whole frequency span and in increments of 0.1 kHz near the fundamental frequency).

3.3. Pulsed operation based on cavity dumping

To shift pulsed operation over to the 2nd slope of the output power characteristic (Fig. 2(b)), we modified the initial pulse-periodic electrical control signal by inverting it and applying +12.5 V bias voltage. Thus, the base level of the modified electrical pulses was set at the voltage which switches the WEOS to the state of strongly suppressed output coupling and the lowest intracavity loss in the laser. Peaks of the inverted electrical pulses were at the +6 V level, thereby providing the pulsed output coupling which yielded (at the WEOS output port 2) a peak laser power close to the highest possible according to the power characteristic in Fig. 2(b). The achieved 2nd-slope pulsed operation was not repetition-rate sensitive as opposed to the above-described mode-locked operation. This is because the operation was shifted to the saturation region of the intracavity laser power where it loses strong correlation with variation of output coupling as follows from Fig. 2(b). Thus, we were able to change the laser pulse repetition rate freely and explored its continuous tuning from 450 kHz to several MHz without any perceptible effect on the pulse shape, duration and amplitude. The way used to trigger the 2nd-slope pulsed operation can be technically attributed to the cavity dumping: the output coupling is enabled only for short-time extraction of laser radiation. In our setup it did not lead to energy boosting (pulse energy remained at ~0.2 nJ), since the SOA cannot store as much energy as long-lifetime active media under cavity dumping [19], but it allowed wide-range continuous adjustment of the pulse repetition rate.

Figure 5 illustrates the measured basic characteristics of laser pulses yielded at different arbitrary repetition rates regardless of the actual cavity length. The laser pulses have duration of 24 ns (at half maximum), thus being slightly shorter than 30-ns control electrical pulses.

Optics EXPRESS

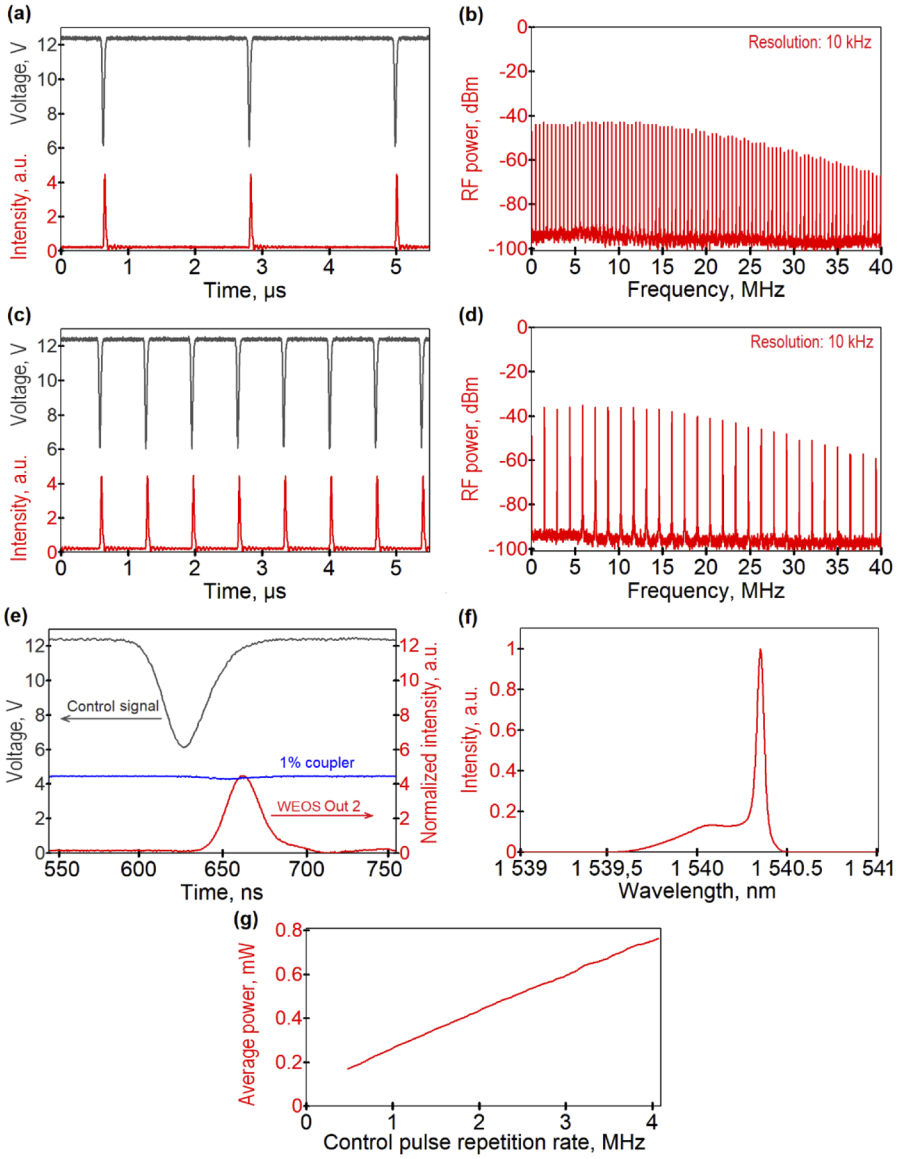

Fig. 5. Measured characteristics of cavity-dumping-based pulsed operation: (a) Oscillogram of electrical control signal (gray trace) and resulting laser pulse train (red trace) with a repetition rate of 459 kHz (2.09 times lower than the fundamental rate imposed by the cavity round trip time); (b) Corresponding RF spectrum of the laser pulse train with the 459 kHz repetition rate; (c) Oscillogram of electrical control signal (gray trace) and resulting laser pulse train (red trace) with a repetition rate of 1459 kHz (1.52 times higher than the fundamental rate); (d) RF spectrum of the laser pulse train with the 1459 kHz repetition rate; (e) Typical high-resolution time traces of electrical control pulse (grey trace), laser pulse from the WEOS output port 2 (red trace), and intensity variation at the 1% port of the reference coupler (blue trace); (f) Optical spectrum of laser radiation (resolution 0.02 nm) in cavity-dumping operation; (g) Dependence of the average laser power outputted by the WEOS on the repetition rate of the electrical control pulses (scanned stepwise in increments of 0.5 kHz).

Optics EXPRESS

The main probable cause of such pulse shortening is nonlinearity of the power-versus-voltage characteristic of the laser (that affects the pulse form factor). RMS amplitude noise was <2.2%. Ringing in the laser pulse tail is due to adding of the external bias voltage source to the control circuit and the consequent impairment of its impedance matching with the WEOS. Proper impedance matching will ensure cleaner output. RF spectra of the obtained laser pulse trains exhibit relatively high signal-to-noise ratios (> 50 dB), comparable with those of the mode-locked operation. It is important to point out that the intracavity laser power (monitored *via* the 1% reference coupler) was almost unaffected by the pulsed output coupling as seen in Fig. 5(e) due to its fast (single pass) recovery in the SOA. Figure 5(g) also indicates the possibility of arbitrary setting and continuous tuning of the pulse repetition rate independently of the cavity round trip time. Continuous adjustment of the pulse repetition rate within the multi-octave range (from 0.45 to 4.1 MHz) only causes the corresponding smooth variation of the average output laser power without affecting other pulse parameters.

4. Discussion

Besides the demonstrated feasibility of the proposed method, our study presented also particular findings which are of practical interest and should be highlighted as follows.

Electronic adjustment of the WEOS complementary transmission characteristics allows taking advantage of lasing under conditions of the varied output coupling. Depending on the variation range, in CW lasing regime, it can cause either well correlated variations of the output and intracavity powers or variation of the output power only (the intracavity power being sustained in saturation as shown in Fig. 2(b)). Besides optimization of the CW lasing performance, the above feature also affords extended capabilities for triggering of essentially different pulsed operations (*i.e.* mode locking and cavity dumping). Moreover, the fast recovery gain provided by SOA grants some advantages to those pulsed regimes: (i) strong suppression of supermode beat noise (Fig. 3(d)) in harmonically mode-locked operation, and (ii) broadband continuous tunability of pulse repetition in operation based on cavity dumping (Fig. 5(g)). In the latter regime, the repetition rate range is determined only by the maximum speed of optical switching. Owing to nanosecond response time of the WEOS, it is possible to establish the range from 0 Hz (single shot) to hundreds of MHz with the shortest pulse duration of few ns (provided that appropriately fast RW AWG with proper impedance matching is applied). Sub-nanosecond laser pulse shaping requires more advanced WEOS and electronics.

It is important to note that the demonstrated cavity-dumped operation is not affected by intracavity relaxation oscillations which may appear in configurations with long-lifetime fiber active media [6]. Nevertheless, it is interesting to consider the potential of the method also for such active media which can store more pump energy in cavity-dumped regime as compared with SOA. The energy capability of a typical Yb-fiber in such pulsed regime can be estimated from the theoretical work [20] (it suggests tens of nJ), while the work [6] indicates pulse energy of few nJ yielded by cavity dumping in an Er-based configuration. Cavity-dumped operation within a rare-earth-doped configuration may require more accurate modulation of WEOS-based output coupling in order to prevent output from intracavity relaxation oscillation. This will be the subject of our further study.

From the application point of view, triggering of mode-locked operation may be useful for tasks related to time-frequency metrology [21] owing to the tight locking of the pulse repetition rate to the cavity round trip time, while the pulsed operation with freely tunable repetition rate can be particularly useful for external-cavity Raman conversion [22] and other laser applications in which synchronous pumping, injection locking, or pulsed seeding requires particular matching in time/frequency domains [23,24]. The method can afford extended capabilities also for triggering of nontrivial pulsed regimes (e.g. pulse patterns and waveforms [12,25] including aperiodic ones). It is also important to note that the spectral bandwidth of the demonstrated pulsed lasing regimes

Optics EXPRESS

is relatively small (of the order of 0.1 nm). Development of stable nanosecond pulsed lasers with ultra-narrow spectral width becomes very topical nowadays [26], because such sources can be particularly useful for spectroscopy [27], efficient excitation of molecules [28], sensing and quantum optics [29].

Besides the unique electronically controllable variability of the lasing regimes and their parameters, the explored method also features an advantage related to the compactness of the fiber cavity lasers: the WEOS can substitute completely for a few intracavity elements (for a fixed output coupler and a modulator in mode-locked operation as well as for a pulse picker in cavity-dumped operation). Thus, it also brings an extra benefit of reduced total intracavity loss. Although laser output power obtained in the present experimental realization was quite moderate, it can be increased with the use of more powerful high-gain SOA components (such as the one reported in [30]). Moreover, the proposed master oscillator can seed efficiently different types of power amplifiers including single-pass erbium-doped, semiconductor and regenerative ones.

The demonstrated method can be further improved by using a faster WEOS for sub-nanosecond pulse generation at repetition rates up to a few GHz.

5. Summary

Employment of a fiber-coupled $LiNbO_3$ waveguide electro-optic switch in the role of the variable output coupler in a fiber cavity laser allows broad-range all-electronic control over the properties of laser generation. In the present work, this is demonstrated on the example of a laser with a low-inertia active medium using SOA. It is shown that WEOS can be used both for active mode locking and for cavity dumping. The latter allows laser pulse repetition rate to be continuously tunable within a multi-octave range spanning the kHz and MHz domains. This is the distinct difference between the presented laser and conventional actively mode-locked fiber lasers whose pulse repetition rate cannot be tuned so freely. Moreover, the cavity-dumped operation of the proposed laser can allow even single shot laser emission. Temporal profile of the emitted laser pulses is fully governed by the control signal applied to the WEOS. Combination of these features opens up prospects to creation of a universal coherent optical waveform generator capable of synthesizing even aperiodic waveforms in contrast to known approaches based on active mode locking [12,25].

The proposed method may be also implemented in lasers with active media based on rare-earth-doped fibers taking advantage of their long-lifetime upper laser levels for cavity-dumped operation. Comparatively simple and reproducible electronic control over WEOS offers unique flexibility for triggering and tuning of essentially different pulsed lasing regimes, thereby materially expanding functionality of fiber lasers, making them more universal and easier controllable.

Funding

Ministry of Science and Higher Education of the Russian Federation (0735-2020-0007); Russian Foundation for Basic Research (18-32-20021, 18-29-20025); Russian Foundation for Basic Research and Novosibirsk Oblast (19-42-540013).

Disclosures

The authors declare no conflicts of interest.

References

1. E. J. Lee, S. Y. Choi, H. Jeong, N. H. Park, W. Yim, M. H. Kim, J.-K. Park, S. Son, S. Bae, S. J. Kim, K. Lee, Y. H. Ahn, K. J. Ahn, B. H. Hong, J.-Y. Park, F. Rotermund, and D.-I. Yeom, "Active control of all-fibre graphene devices with electrical gating," Nat. Commun. **6**(1), 6851 (2015).

Optics EXPRESS

2. Y. Gladush, A. A. Mkrtchyan, D. S. Kopylova, A. Ivanenko, B. Nyushkov, S. Kobtsev, A. Kokhanovskiy, A. Khegai, M. Melkumov, M. Burdanova, M. Staniforth, J. Lloyd-Hughes, and A. G. Nasibulin, "Ionic liquid gated carbon nanotube saturable absorber for switchable pulse generation," Nano Lett. **19**(9), 5836–5843 (2019).
3. M. Bello-Jiménez, C. Cuadrado-Laborde, A. Díez, J. L. Cruz, M. V. Andrés, and A. Rodríguez-Cobos, "Mode-locked all-fiber ring laser based on broad bandwidth in-fiber acousto-optic modulator," Appl. Phys. B **110**(1), 73–80 (2013).
4. J. Kim, J. Koo, and J. H. Lee, "All-fiber acousto-optic modulator based on a cladding-etched optical fiber for active mode-locking," Photonics Res. **5**(5), 391–395 (2017).
5. J. M. Roth, K. Dreyer, B. C. Collings, W. H. Knox, and K. Bergman, "Actively mode-locked 1.5-μm 10-GHz picosecond fiber laser using a monolithic semiconductor optical amplifier/electroabsorption modulator," IEEE Photonics Technol. Lett. **14**(7), 917–919 (2002).
6. M. Malmström, Z. Yu, W. Margulis, O. Tarasenko, and F. Laurell, "All-fiber cavity dumping," Opt. Express **17**(20), 17596–17602 (2009).
7. R. C. Alferness, "Optical guided-wave devices," Science **234**(4778), 825–829 (1986).
8. D. Janner, D. Tulli, M. Belmonte, and V. Pruneri, "Waveguide electro-optic modulation in micro-engineered $LiNbO_3$," J. Opt. A: Pure Appl. Opt. **10**(10), 104003 (2008).
9. T. S. El-Bawab, *Optical Switching* (Springer, 2006).
10. Y. Liao, H. Zhou, and Z. Meng, "Modulation efficiency of a $LiNbO_3$ waveguide electro-optic intensity modulator operating at high microwave frequency," Opt. Lett. **34**(12), 1822–1824 (2009).
11. R. Wang, Y. Dai, L. Yan, J. Wu, K. Xu, Y. Li, and J. Lin, "Dissipative soliton in actively mode-locked fiber laser," Opt. Express **20**(6), 6406–6411 (2012).
12. B. N. Nyushkov, S. M. Kobtsev, A. V. Ivanenko, and S. V. Smirnov, "Programmable optical waveform generation in a mode-locked gain-modulated SOA-fiber laser," J. Opt. Soc. Am. B **36**(11), 3133–3138 (2019).
13. Z. Zhang, J. Wu, K. Xu, X. Hong, and J. Lin, "Tunable multiwavelength SOA fiber laser with ultra-narrow wavelength spacing based on nonlinear polarization rotation," Opt. Express **17**(19), 17200–17205 (2009).
14. W. H. Press, S. A. Teukolsky, W. T. Vetterling, and B. P. Flannery, *Numerical Recipes in C++* (Cambridge University, 2007), Chap. 9.
15. O. Pottiez, O. Deparis, R. Kiyan, M. Haelterman, P. Emplit, P. Megret, and M. Blondel, "Supermode noise of harmonically mode-locked erbium fiber lasers with composite cavity," IEEE J. Quantum Electron. **38**(3), 252–259 (2002).
16. C. Peng, M. Yao, Q. Xu, and H. Zhang, "Suppression of supermode competitions in SOA fiber mode-locked ring laser," *The 15th Annual Meeting of the IEEE Lasers and Electro-Optics Society*, Glasgow, UK, 2002, pp. 377–378 vol.2.
17. G.-R. Lin, M.-C. Wu, Y.-C. Chang, and C.-L. Pan, "Ultrahigh supermode noise suppressing ratio of a semiconductor optical amplifier filtered harmonically mode-locked Erbium-doped fiber laser," Opt. Express **13**(18), 7215–7224 (2005).
18. C. Wu and N. K. Dutta, "High-repetition-rate optical pulse generation using a rational harmonic mode-locked fiber laser," IEEE J. Quantum Electron. **36**(6), 721–727 (2000).
19. J. Myers, C. Kokoczka, G. Cook, and R. Bedford, "High peak power cavity dumping semiconductor lasers," Opt. Lett. **42**(1), 113–116 (2017).
20. O. Shtyrina, A. Kokhanovskiy, I. Yarutkina, A. Skidin, A. Ivanenko, S. Efremov, B. Nyushkov, S. Smirnov, and M. Fedoruk, "Study of gain efficiency in quasi-distributed amplification systems," Opt. Lett. **45**(2), 499–502 (2020).
21. T. Fortier and E. Baumann, "20 years of developments in optical frequency comb technology and applications," Commun. Phys. **2**(1), 153 (2019).
22. S. Kobtsev, A. Ivanenko, A. Kokhanovskiy, and M. Gervaziev, "Raman-converted high-energy double-scale pulses at 1270 nm in P_2O^5-doped silica fiber," Opt. Express **26**(23), 29867–29872 (2018).
23. M. Margalit, M. Orenstein, and G. Eisenstein, "High-repetition-rate mode-locked Er-doped fiber lasers by harmonic injection locking," Opt. Lett. **20**(17), 1791–1793 (1995).
24. C.-G. Jeon, S. Zhang, J. Shin, and J. Kim, "Highly tunable repetition-rate multiplication of mode-locked lasers using all-fibre harmonic injection locking," Sci. Rep. **8**(1), 13875 (2018).
25. B. Nyushkov, A. Ivanenko, S. Smirnov, and S. Kobtsev, "Electronically controlled generation of laser pulse patterns in a synchronously pumped mode-locked semiconductor optical amplifier-fiber laser," Laser Phys. Lett. **16**(11), 115103 (2019).
26. M. Kues, C. Reimer, B. Wetzel, P. Roztocki, B. E. Little, S. T. Chu, T. Hansson, E. A. Viktorov, D. J. Moss, and R. Morandotti, "Passively mode-locked laser with an ultra-narrow spectral width," Nat. Photonics **11**(3), 159–162 (2017).
27. J. Mandon, G. Guelachvili, and N. Picque, "Fourier transform spectroscopy with a laser frequency comb," Nat. Phys. **3**(2), 99–102 (2009).
28. G. Wrigge, I. Gerhardt, J. Hwang, G. Zumofen, and V. Sandoghdar, "Efficient coupling of photons to a single molecule and the observation of its resonance fluorescence," Nat. Phys. **4**(1), 60–66 (2008).
29. C. Reimer, M. Kues, P. Roztocki, B. Wetzel, F. Grazioso, B. E. Little, S. T. Chu, T. Johnston, Y. Bromberg, L. Caspani, D. J. Moss, and R. Morandotti, "Generation of multiphoton entangled quantum states by means of integrated frequency combs," Science **351**(6278), 1176–1180 (2016).

Optics EXPRESS

30. K. V. Gasse, R. Wang, and G. Roelkens, "27 dB gain III–V-on-silicon semiconductor optical amplifier with > 17 dBm output power," Opt. Express **27**(1), 293–302 (2019).